arXiv:0809.3426v1 [cond-mat.other] 19 Sep 2008

Superfluid and Fermi liquid phases of Bose-Fermi mixtures in optical lattices

Kaushik Mitra, C. J. Williams and C. A. R. Sá de Melo
Joint Quantum Institute, University of Maryland, College Park, Maryland 20742,
and National Institute of Standards and Technology, Gaithersburg, Maryland 20899
(Dated: September 19, 2008)

We describe interacting mixtures of ultracold bosonic and fermionic atoms in harmonically confined optical lattices. For a suitable choice of parameters we study the emergence of superfluid and Fermi liquid (non-insulating) regions out of Bose-Mott and Fermi-band insulators, due to finite Boson and Fermion hopping. We obtain the shell structure for the system and show that angular momentum can be transferred to the non-insulating regions from Laguerre-Gaussian beams, which combined with Bragg spectroscopy can reveal all superfluid and Fermi liquid shells.

PACS numbers: 03.75.Hh, 03.75.Kk, 03.75 Lm

Fermi and Bose degenerate quantum gases and liquids are amazing systems, which have revealed individually several macroscopic quantum phenomena. For instance, superfluidity is known to exist in neutral liquids such as ^{4}He (boson) and in ^{3}He (fermion), as well as in a variety of electronic materials studied in standard condensed matter physics. The role of quantum statistics and interactions is of fundamental importance to understand the phases emerging from purely bosonic or purely fermionic systems, and a substantial amount of understanding of these individual Bose or Fermi systems can be found in the atomic and condensed matter physics literature. However, new frontiers can be explored when mixtures of bosons and fermions are produced in harmonic traps or optical lattices. An important example of the richness of quantum degenerate Bose-Fermi mixtures was revealed in standard condensed matter systems, where for fixed ^{4}He density and increasing amounts of ^{3}He, the critical temperature for superfluidity is reduced, and below a tricritical point phase separation appears [1]. In this Bose-Fermi mixture of standard condensed matter physics, essentially the only control parameter is the ratio between the densities of ^{4}He and ^{3}He.

In atomic physics, a spectacular degree of control has been achieved in Bose-Fermi mixtures, where not only the ratio between densities of bosons and fermions can be adjusted, but also the interactions between fermions and bosons can be controlled through the use of Feshbach resonances [2], as demonstrated in mixtures of harmonically trapped Bose-Fermi polarized Fermion mixtures of ^{40}K and ^{87}Rb. Furthermore, these same atoms have been succesfully loaded into optical lattices [3] and have produced a system that has no counterpart in standard condensed matter systems. By controlling the depths of optical lattices we can change not only the interactions between boson and fermions, but also their hopping from site to site, thus allowing the exploration of a very rich phase space, where supersolid and phase separated states have been suggested [4]. The list of Bose-Fermi mixtures in atomic physics is growing, and include systems where the masses are close like ^{6}Li and ^{7}Li, ^{39}K and ^{40}K, or ^{172}Yb and ^{173}Yb; or systems where the masses are quite different like ^{6}Li and ^{40}K, ^{7}Li and ^{39}K, ^{6}Li and ^{23}Na, ^{6}Li and ^{87}Rb, ^{40}K and ^{23}Na, or ^{40}K and ^{87}Rb. This suggests a wide possibility of regimes that can be reached by tuning interactions, density and geometry, which is not is possible in ordinary condensed matter physics.

A few studies of quantum phases of Bose-Fermi mixtures have focused on homogeneous three dimensional systems with [6, 7], and without optical lattices [5]. However, only one effort focused on harmonically confined optical lattices [8]. Most of the descriptions of Bose-Fermi mixtures in optical lattices have relied on numerical methods using either Gutzwiller projection [6, 8] or quantum Monte Carlo [7] techniques. In this paper, we present a fully analytical theory of boson and spin polarized fermion mixtures in harmonically confined optical lattices by using degenerate perturbation theory for finite hopping in conjunction with the local density approximation. This work provides insight into the phase diagram of Bose-Fermi mixtures, and into the detection of superfluid and Fermi liquid shells at low temperatures.

This paper we analyses in detail the regime where the hopping parameters of bosons and fermions are comparable and the repulsion between bosons and fermions is a substantial fraction of the boson-boson repulsion. In this case, the system presents regions of (I) coexisting Bose-Mott and Fermi-band insulator, (II) coexisting Bose-Mott insulator and Fermi liquid, (III) Bose-Mott insulator, and (IV) Bose superfluid, as shown in Fig. 1. We compute analytically the boundaries between various phases, and obtain the spatially dependent boson and fermions filling fractions in each region. Although one can envisage other situations where, for example, one can have coexistence of superfluid and Fermi band insulator, we confine our discussion to the situation above for the sake of simplicity. Finally, we propose a detection method of the shell strucuture of Bose-Fermi mixtures by using Laguerre-Gaussian beams [9] and Bragg spectroscopy [10], where angular momentum is transferred only to regions with extended states such as the superfluid and Fermi-liquid shells.

To describe Bose-Fermi mixtures in harmonically confined square (2D) or cubic (3D) optical lattices we start with the Hamiltonian

$$\hat{H} = K_B + K_F - \sum_{\mathbf{r}} \mu_B(\mathbf{r})\hat{n}_B(\mathbf{r}) - \sum_{\mathbf{r}} \mu_F(\mathbf{r})\hat{n}_F(\mathbf{r}) + \frac{U_{BB}}{2}\sum_{\mathbf{r}} \hat{n}_B(\mathbf{r})\left[\hat{n}_B(\mathbf{r})-1\right] + U_{BF}\sum_{\mathbf{r}} \hat{n}_B(\mathbf{r})\hat{n}_F(\mathbf{r}),$$

where $K_B = -t_B \sum_{\langle \mathbf{r},\mathbf{r}'\rangle} b^\dagger_{\mathbf{r}} b_{\mathbf{r}'}$ and $K_F = -t_F \sum_{\langle \mathbf{r},\mathbf{r}'\rangle} f^\dagger_{\mathbf{r}} f_{\mathbf{r}'}$ are the kinetic energies of boson and fermions with nearest-neighbor hoppings t_B and t_F, and $b^\dagger_{\mathbf{r}}$ and $f^\dagger_{\mathbf{r}}$ are the bosonic and fermionic creation operators at site $\mathbf{r}$. Here, the lattice sites for bosons and fermions are assumed to be the same, but the hopping parameters can be different. The number operators are $\hat{n}_B(\mathbf{r}) = b^\dagger_{\mathbf{r}} b_{\mathbf{r}}$ and $\hat{n}_F(\mathbf{r}) = f^\dagger_{\mathbf{r}} f_{\mathbf{r}}$, and the corresponding local chemical potentials are $\mu_F(\mathbf{r}) = \mu_F - V_F(\mathbf{r})$ and $\mu_B(\mathbf{r}) = \mu_B - V_B(\mathbf{r})$, where $V_F(\mathbf{r}) = \Omega_F(r/a)^2/2$ and $V_B(\mathbf{r}) = \Omega_B(r/a)^2/2$ are the harmonically confining potentials and μ_F and μ_B are the chemical potentials for fermions and bosons. The origin of the lattice with spacing a is chosen to be at the minimum of the harmonically confining potential. The terms containing U_{BB} (U_{BF}) represent the boson-boson (boson-fermion) interaction.

When $t_B = t_F = 0$, the Hamiltonian $\hat{H} = \hat{H}_0$ is a sum of single-site contributions, and the eigenstates are tensor products of number states with state vectors $|\psi\rangle = |n_{B,0}, n_{B,1}, \cdots\rangle |n_{F,0}, n_{F,1}, \cdots\rangle$, with $n_{B,\mathbf{r}} = 0, 1, 2, ...$ and $n_{F,\mathbf{r}} = 0, 1$ representing the occupation number of bosons and fermions at site $\mathbf{r}$, respectively. At site $\mathbf{r}$ the local energy is $E_{n_B,n_F}(\mathbf{r}) = U_{BB} n_B(n_B - 1)/2 + U_{BF} n_B n_F - \mu_B(\mathbf{r}) n_B - \mu_F(\mathbf{r}) n_F$. For the ground state wavefunction the number of bosons at site $\mathbf{r}$ is determined by $max(0, \lfloor (U_{BB} + \mu_B(\mathbf{r}))/2U_{BB} \rfloor)$ if $E_{n_B,0}(\mathbf{r}) < E_{n_B,1}(\mathbf{r})$ and $max(0, \lfloor (U_{BB} + \mu_B(\mathbf{r}) - U_{BF})/2U_{BB} \rfloor)$ otherwise. Similarly, the number of fermions per site is zero if $E_{n_B,0}(\mathbf{r}) < E_{n_B,1}(\mathbf{r})$ and one otherwise. The symbol $\lfloor \cdot \rfloor$ is the floor function. In the ground state solution shells (n_B, n_F) with n_B bosons and n_F fermions are formed by those lattice sites $\mathbf{r}$ for which the local energy is the same. For our harmonic traps these shells are nearly spherically symmetric. The boundary between shells (n_B, n_F) and $(n_B + 1, n_F)$ is determined by $E_{n_B,n_F}(\mathbf{r}) = E_{n_B+1,n_F}(\mathbf{r})$, leading to the radius $R_{B,n_B,n_F} = a\sqrt{\Omega_{n_B,n_F}/\Omega_B}$, where $\Omega_{n_B,n_F} = 2(\mu_B - n_B U_{BB} - n_F U_{BF})$. Similarly, the boundary between shells with occupation numbers $(n_B, 0)$ and $(n_B, 1)$ is determined by equating the local energies $E_{n_B,n_F}(\mathbf{r})$ and $E_{n_B,n_F+1}(\mathbf{r})$, leading to the radius $R_{F,n_B} = a\sqrt{2(\mu_F - n_B U_{BF})/\Omega_F}$. We consider the number of particles to be sufficiently large such that the radii of the boundaries are much larger than a.

Next, we begin our discussion of finite hoppings by taking first $t_B \neq 0$, with $t_F = 0$. The Bose superfluid region emerges due to kinetic fluctuations at the boundaries between the (n_B, n_F) and $(n_B + 1, n_F)$ shells. At this boundary the local energy $E_{n_B+1,n_F}(\mathbf{r})$ is degenerate with $E_{n_B,n_F}(\mathbf{r})$. To describe the emergence of superfluid regions, we introduce the order parameter for superfluidity $\psi_{B,j}$ via the transformation $b^\dagger_i b_j \rightarrow \psi^*_{B,i} b_j + b^\dagger_i \psi_{B,j} - \psi^*_{B,i}\psi_{B,j}$, and then for analytical convenience make the continuum approximation $\psi(\mathbf{r} + a) = \psi(\mathbf{r}) + a_i \partial_i \psi(\mathbf{r}) + (1/2) a_i a_j \partial_i \partial_j \psi(\mathbf{r})$.

In the limit of $U_{BB} \gg t_B$, we can restrict our Hilbert space to the number basis states $|n_B, n_F\rangle$ and $|n_B + 1, n_F\rangle$, as any contribution from other basis states to the local energy is of order t_B^2/U_{BB}. The hopping term t_B affects the energies $E_{n_B+1,n_F}(\mathbf{r})$ and $E_{n_B,n_F}(\mathbf{r})$ by removing their degeneracy, thus creating finite-width superfluid regions between shells (n_B+1, n_F) and (n_B, n_F). The effective local Hamiltonian then becomes,

$$H^{\text{eff}}_{\mathbf{r}} = \begin{pmatrix} E_{n_B,n_F}(\mathbf{r}) + \Lambda(\mathbf{r}) & -\sqrt{n_B+1}\Delta(\mathbf{r}) \\ -\sqrt{n_B+1}\Delta^*(\mathbf{r}) & E_{n_B+1,n_F}(\mathbf{r}) + \Lambda(\mathbf{r}) \end{pmatrix}, \tag{1}$$

where $\Lambda(\mathbf{r}) = \frac{1}{2}(\Delta(\mathbf{r})\psi^*(\mathbf{r}) + cc)$ and $\Delta(\mathbf{r}) = t_B(z\psi(\mathbf{r}) + a^2\nabla^2\psi(\mathbf{r}))$. Here, z is the coordination number which depends on the lattice dimension d.

The eigenvalues of Eq. (1) are given by,

$$E_\pm(\mathbf{r}) = E_s(\mathbf{r}) \pm \sqrt{\left[E_d(\mathbf{r})\right]^2 + (n_B+1)\left|\Delta(\mathbf{r})\right|^2},$$

where $E_s(\mathbf{r}) = \left[E_{n_B+1,n_F)}(\mathbf{r}) + E_{n_B,n_F}(\mathbf{r})\right]/2 + \Lambda(\mathbf{r})$ is proportional to the sum of the diagonal terms, and $E_d(\mathbf{r}) = \left[E_{n_B+1,n_F}(\mathbf{r}) - E_{n_B,n_F}(\mathbf{r})\right]/2 = (n_B U_{BB} + n_F U_{BF} - \mu_B(\mathbf{r})/2$ is proportional to their difference. Notice that $E_-(\mathbf{r})$ is the lowest local energy leading to the total ground state energy $\mathbf{E} = \frac{1}{L^d}\int d\mathbf{r} E_-(\mathbf{r})$.

The order parameter equation (OPE) is determined by minimization of $\mathbf{E}$ with respect to $\psi^*(\mathbf{r})$ leading to

$$\Delta(\mathbf{r}) - \frac{(n_B+1)t_B(z + a^2\nabla^2)\Delta(\mathbf{r})}{2\sqrt{\left|E_d(\mathbf{r})\right|^2 + (n_B+1)\left|\Delta(\mathbf{r})\right|^2}} = 0. \tag{2}$$

Notice that the OPE is not of the Gross-Pitaeviskii (GP) type, since the superfluid regions emerge from local fluctuations between neighboring Mott shells. Ignoring the spatial derivatives of ψ in Eq. 2 leads to the spatially dependent order parameter

$$\left|\psi(\mathbf{r})\right|^2 = \frac{n_B+1}{4} - \frac{\left(n_B U_{BB} + n_F U_{BF} - \mu_B(\mathbf{r})\right)^2}{4z^2 t_B^2 (n_B+1)}. \tag{3}$$

Since $\left|\psi(\mathbf{r})\right|^2 \geq 0$, hence $|n_B U_{BB} + n_F U_{BF} - \mu_{B,\mathbf{r}}| \leq (n_B+1) z t_B$, and the inner $R_{n_B,n_F,-}$ and outer $R_{n_B,n_F,+}$ radii for the superfluid shell between the (n_B, n_F) and $(n_B + 1, n_F)$ Mott regions are obtained by setting $\left|\psi(\mathbf{r})\right|^2 = 0$ leading to

$$R_{n_B,n_F,\pm} = R_{B,n_B,n_F}\sqrt{1 \pm \frac{2zt_B(n_B+1)}{\Omega_B}\frac{a^2}{R^2_{B,n_B,n_F}}}.$$

This relation shows explicitly that t_B splits the spatial degeneracy of the (n_B, n_F) and (n_B+1, n_F) insulating shells at $r = R_{c,n_B,n_F}$ or $\mu_B(\mathbf{r}) = n_B U_B B + n_F U_{BF}$ by introducing a superfluid region of width $\Delta R_{n_B,n_F} = R_{n_B,n_F,+} - R_{n_B,n_F,-}$. (See Fig. 1 for characteristic widths).

In addition, the local bosonic filling fraction

$$n_B(\mathbf{r}) = -\frac{\partial E_-(\mathbf{r})}{\partial \mu_B} = n_B + \frac{1}{2} - \frac{n_B U_{BB} + n_F U_{BF} - \mu_B(\mathbf{r})}{2zt_B(n_B+1)}$$

in the same region interpolates between $n_B + 1$ for $r \lesssim R_{n_B,n_F,-}$ and n for $r \gtrsim R_{n_B,n_F,+}$, while the chemical potential μ_B is fixed by the total number of bosons $N_B = \int d\mathbf{r} n(\mathbf{r})$. The local bosonic compressibility $\kappa_B(\mathbf{r}) = \partial n_B(\mathbf{r})/\partial \mu_B = 1/2zt_B(n_B+1)$ of the superfluid shells is non-zero, in contrast to the incompressible $(\kappa_B = 0)$ (n_B, n_F) and (n_B+1, n_F) insulating shells for $r < R_{n_B,n_F,-}$ and $r > R_{n_B,n_F,+}$, respectively.

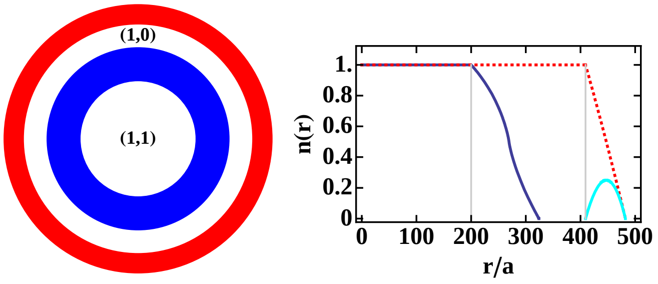

FIG. 1: (color online) (a) Shell structure of Bose-Fermi mixtures in harmonically confined optical lattices showing a coexisting Bose-Mott and Fermi-band insulator region at the center $(n_B = 1, n_F = 1)$, a coexisting Bose-Mott insulator and Fermi liquid region (in blue), a Bose-Mott insulator region $(n_B = 1, n_F = 0)$, and Bose-Superfluid region at the edge (in red). (b) filling factors for fermions shown as the solid (dark blue) curve and for bosons shown at the dashed (red) curve. The solid parabolic curve (light blue) shows the order parameter in the superfluid region. The parameters used are $t_F = t_B = 0.0325 U_{BB}$, $U_{BF} = 0.1 U_{BB}$, $\mu_B = 0.8 U_{BB}$, $\mu_F = 0.4 U_{BB}$ and $\Omega_F = \Omega_B = 8 \times 10^{-6} U_{BB}$, which are representative of Bose-Fermi mixtures with nearly the same mass such as ^{6}Li and ^{7}Li, ^{39}K and ^{40}K, or ^{172}Yb and ^{173}Yb. For the parameters chosen, the widths of the superfluid and FL shells are several times larger than the lattice spacing a.

Now, we consider finite t_F. In order to have a tractable theory we assume that the shell boundaries of the bosons and fermions are well separated. This allows us to investigate the Fermi liquid near the shell boundary of the fermions in the presence of a Bose-Mott insulator with n_B bosons per site. Furthermore, if we assume that the local density of the Fermi gas is smoothly varying then the local number of fermions is

$$n_F(\mathbf{r}) = \int_{\epsilon_{\min}}^{\epsilon_{\max}} d\epsilon \mathcal{D}(\epsilon) f[\epsilon - \mu_F^{\text{eff}}(\mathbf{r})] \qquad (4)$$

where $f[x]$ is the Fermi function at temperature T, and $\mathcal{D}(\epsilon) = \sum_{\mathbf{k}} \delta(\epsilon - \epsilon_{\mathbf{k}})$ is the density of fermion states with energy dispersion $\epsilon_{\mathbf{k}} = -2t_F \sum_\ell^d \cos(k_\ell a)$. The effective chemical potential $\mu_F^{\text{eff}}(\mathbf{r}) = \mu_F(\mathbf{r}) - n_B U_{BF}$ accounts for the effect of the bosons. The band minimum and maximum of $\epsilon_{\mathbf{k}}$ are $\epsilon_{\min} = -2dt_F$ and $\epsilon_{\max} = 2dt_F$, respectively. Thus, the Fermi liquid region is limited by the boundaries $\epsilon_{\min} \leq \mu_F(\mathbf{r}) \leq \epsilon_{\max}$, leading to $R_{F,\pm} = R_{F,n_B}\sqrt{1 \pm 2zt_F a^2/\Omega_F R_{F,n_B}^2}$ for the inner $R_{F,-}$ and outer $R_{F,+}$ radius of the FL shell. The width of the FL region is $\Delta R_{F,n_B} = R_{F,+} - R_{F,-}$. (See Fig. 1 for characteristic widths). The isothermal compressibility of the FL region is $\kappa_F(\mathbf{r}) = \partial n_F(\mathbf{r})/\partial \mu_F$, which leads at zero temperature to $\kappa_F(\mathbf{r}) = 0$ outside the FL shell, indicating the presence of insulating regions and $\kappa_F(\mathbf{r}) = \mathcal{D}[\mu_F(\mathbf{r})]$ inside the FL shell, indicating the presence of conducting regions. The superfluid and FL shells for finite t_B and t_F, and their density profiles are shown in Fig. 1 for the two-dimensional case.

Next, we propose an experiment to detect superfluid and Fermi liquid shells in Bose-Fermi mixtures using a combination of Gaussian and Laguerre-Gaussian beams followed by Bragg spectroscopy. To illustrate the idea, we discuss the simpler case of a nearly two-dimensional configuration, where the harmonic trap is very tight along the z-direction, loose along the x- and y- directions. Upon application of Gaussian and Laguerre-Gaussian beams along the z-direction, only angular momentum is transferred to the atoms in the conducting phases (superfluid or Fermi liquid), imposing a rotating current with a well defined velocity profile, while the insulating regions do not absorb angular momentum due to their large gap in the excitation spectrum.

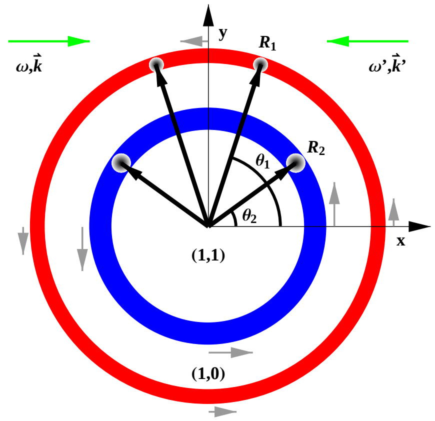

FIG. 2: (Color online) Schematic plot for the detection of outer (red) superfluid and inner (blue) Fermi liquid shells using Bragg spectroscopy. The angles θ_1 and θ_2 indicate the locations of strongest momentum transfer from the Bragg beams (large green arrows) to the rotating superfluid and Fermi liquid shells of radii R_1 and R_2. The gray arrows indicate the sense of rotation of the conducting shells.

To probe the rotating superfluid and Fermi liquid phases we propose the use of two counter-propagating

Bragg beams applied in the xy plane along the x direction, as indicated in Fig. 2.

The Bragg beams transfer a net linear momentum $\hbar(k+k')\mathbf{x}$ to the atoms of mass m which satisfy the energy conservation condition

$$\hbar(\omega-\omega') = \epsilon_f - \epsilon_i - v_x\hbar(k+k') + \frac{\hbar^2(k+k')^2}{2m}, \quad (5)$$

where v_x is the component of the velocity $\mathbf{v}(\mathbf{r}) = \mathbf{p}(\mathbf{r})/m$ along the x direction and ϵ_i and ϵ_f are the experimentally accessible energies of the initial and final internal states atom. For an atom carrying one unit of angular momentum, the velocity is $\mathbf{v}_i = \hbar\hat{\theta}/mr$. Therefore, within a conducting shell with radius $r = R$ atoms get a linear momentum kick of $\hbar(k+k')\hat{\mathbf{x}}$ when the velocity $v_x = \hbar\sin\theta/mR$ satisfies the condition given in Eq. 5. This leads to two Bragg angles $\theta = -\sin^{-1}(mRv_x/\hbar)$, and $\pi-\theta$ for each conducting shell. As can be seen in Fig. 2, the Bragg angles are θ_1 and $\pi-\theta_1$ for the outer superfluid shell labelled by R_1, and are θ_2 and $\pi-\theta_2$ for the fermi liquid shell labelled by R_2. Once these atoms are kicked out of the conducting shells, they form two small expanding clouds, which can be detected by direct absorption imaging.

Next, we discuss the time scales over which the rotation in the conducting regions persist and can be detected experimentally. In the case of the superfluid region we use the Landau criterion to show that the velocity imposed to the superfluid through the angular momentum transfer is much smaller than the local sound velocity $c(\mathbf{r}) = \sqrt{\rho_s(\mathbf{r})/\kappa}$, where $\rho_s(\mathbf{r}) = 2t_B a^2|\psi(\mathbf{r})|^2$ is the local superfluid density, and κ is the compressibility. Thus, $c(\mathbf{r}) = 2\sqrt{(n_B+1)zta}|\psi(\mathbf{r})|$ vanishes at the insulator boundaries where $|\psi(\mathbf{r})| = 0$, and only close to the edge of the superfluid regions the local rotational speed $v(\mathbf{r}) = \hbar/mr$ exceeds $c(\mathbf{r})$, which means that essentially all the superfluid region can be detected and the angular momentum transferred does not decay over time scales of at least seconds, limited by the lifetime of the trapped system.

In the case of the Fermi liquid region, the time scale over which the flow of the fermions persist in presence of the Bose-Mott insulator background can be calculated from the imaginary part of the fermionic self-energy

$$\Sigma_F(k) = U_{BF}^2 T^2 \sum_{q_1,q_2} G_B(q_1)G_B(q_2)G_F(k+q_1-q_2),$$

where $k = (\mathbf{k}, i\omega)$ and $q_i = (\mathbf{q}_i, i\nu_i)$, with ω (ν_i) are fermionic (bosonic) Matsubara frequencies and T is temperature. The bare inverse bosonic propagator in the Bose-Mott phase is

$$G_B^{-1}(q,\mathbf{r}) = \epsilon_{\mathbf{q}}\left[1+\epsilon_{\mathbf{q}}\left(\frac{n_B+1}{i\hbar\omega - E_1(\mathbf{r})} - \frac{n_B}{i\hbar\omega - E_2(\mathbf{r})}\right)\right],$$

where $E_1(\mathbf{r}) = (n_B-1)U_{BB} - \mu_B(\mathbf{r})$, $E_2(\mathbf{r}) = (n_B-2)U_{BB} - \mu_B(\mathbf{r})$ and $\epsilon_{\mathbf{q}} = -2t_B\sum_\ell^d \cos(k_\ell a)$. The bare inverse fermionic propagator in the Fermi liquid phase is $G_F^{-1}(k,\mathbf{r}) = i\hbar\omega - \epsilon_F(\mathbf{k},\mathbf{r})$, where $\epsilon_F(\mathbf{k},\mathbf{r}) = \epsilon_F(\mathbf{k}) - \mu_F(\mathbf{r})$. For $n_B = 1$ and $T = 0$, the imaginary part of the fermionic self-energy is

$$\mathrm{Im}\Sigma_F(k,\mathbf{r}) = -\pi U_{BF}^2\left[F(\hbar\omega) + F(-\hbar\omega)\right], \quad (6)$$

where $F(\hbar\omega) = \Theta(\hbar\omega)\Theta(-\hbar\omega+\mu_B(\mathbf{r}))\mathcal{D}(\hbar\omega+\mu_F(\mathbf{r}))$, Θ is the Heaviside step function, and $\mathcal{D}(\epsilon)$ is the Fermion density of states. For a two-dimensional Fermi liquid shell, there is a Van Hove singularity in $\mathcal{D}(\epsilon)$ at half filling. The expression in Eq. (6) is independent of momentum, since the dominant excitations in the Bose-Mott region are number-conserving and low-momentum particle-hole excitations, but strongly dependent on position through $\mu_B(\mathbf{r})$ and $\mu_F(\mathbf{r})$, leading to a characteristic decay time $\tau_{\mathbf{r}} = -h/\mathrm{Im}\Sigma(k,\mathbf{r})$. For the parameters used in Fig. 1, (with $U_{BF}/h = 1$ kHz) the time scale for the persistence of the flow near the edges (away from the Van Hove singularity) is $\tau_{\mathbf{r}} \approx 13$ ms. However, near the center of the Fermi liquid region (close to the Van Hove singularity) $\tau_{\mathbf{r}}$ is extremely short, indicating that it is much easier to detect fermions at the edge than at the center of Fermi liquid shells.

We have discussed the phase diagram of Bose-Fermi mixtures in harmonically confined optical lattices in the regime where the hopping parameters of bosons and fermions are comparable and the repulsion between bosons and fermions is a substantial fraction of the boson-boson repulsion. We showed that the system exhibits regions of (I) coexisting Bose-Mott and Fermi-band insulator, (II) coexisting Bose-Mott insulator and Fermi liquid, (III) Bose-Mott insulator, and (IV) Bose-superfluid. We have calculated analytically the boundaries between these phases and obtained the spatially dependent filling fraction for each region. Finally, we proposed a detection method of the superfluid and Fermi liquid shells of Bose-Fermi mixtures by using Gaussian and Laguerre-Gaussian beams followed by Bragg spectroscopy.

[1] E. H. Graf, D. M. Lee, and J. D. Reppy, Phys. Rev. Lett. **19**, 417 (1967).

[2] S. Ospelkaus *et al.*, Phys. Rev. Lett. **97**, 120403 (2006).

[3] K. Günter *et al.*, Phys. Rev. Lett. **96** 180402 (2006).

[4] H. P. Büchler and G. Blatter, Phys. Rev. Lett. **91**, 130404 (2003).

[5] L. Viverit, C. J. Pethick, and H. Smith, Phys. Rev. A **A**, 053605 (2000).

[6] M. Lewenstein *et al.*, Phys. Rev. Lett. **92**, 050401 (2004).

[7] F. Hébert *et al.*, Phys. Rev. A **76**, 043619 (2007).

[8] M. Cramer, J. Eisert, and F. Illuminati, Phys. Rev. Lett. **93**, 190405 (2004).

[9] C. Ryu *et al.*, Phys. Rev. Lett. **99**, 260401 (2007).

[10] S. R. Muniz, D. S. Naik, and C. Raman, Phys. Rev. A **73** 041605(R) (2006).